



HAL
open science

Experimental results of an organic rankine cycle (ORC) associated to a passive heat removal system for advanced pressurized water reactors (PWR)

Guillaume Lhermet, Nicolas Tauveron, Nadia Caney, Franck Morin

► To cite this version:

Guillaume Lhermet, Nicolas Tauveron, Nadia Caney, Franck Morin. Experimental results of an organic rankine cycle (ORC) associated to a passive heat removal system for advanced pressurized water reactors (PWR). ICAPP2023 - International Congress on Advances in Nuclear Power Plants, ANS, Apr 2023, Gyeongju, South Korea. pp.189. cea-04389217

HAL Id: cea-04389217

<https://cea.hal.science/cea-04389217v1>

Submitted on 11 Jan 2024

HAL is a multi-disciplinary open access archive for the deposit and dissemination of scientific research documents, whether they are published or not. The documents may come from teaching and research institutions in France or abroad, or from public or private research centers.

L'archive ouverte pluridisciplinaire **HAL**, est destinée au dépôt et à la diffusion de documents scientifiques de niveau recherche, publiés ou non, émanant des établissements d'enseignement et de recherche français ou étrangers, des laboratoires publics ou privés.

EXPERIMENTAL RESULTS OF AN ORGANIC RANKINE CYCLE (ORC) ASSOCIATED TO A PASSIVE HEAT REMOVAL SYSTEM FOR ADVANCED PRESSURIZED WATER REACTORS (PWR)

Guillaume Lhermet ^{1,2}, Nicolas Tauveron ², Nadia Caney ² and Franck Morin ¹

¹ CEA, DES, IRESNE, DER, SESI, LCOS, F-13108 Saint Paul Lez Durance, France

² Université Grenoble Alpes, F-38000 Grenoble, France, CEA, LITEN, LCST, F-38054 Grenoble, France

Abstract – *This work concerns a specific passive system design for advanced pressurized water reactor (PWR). The studied system first relies on passive safety condensers, which are increasingly being used in the design of new generation nuclear power plants (NPP). These condensers are typically immersed in large water tanks that function as a cold source or heat sink. They have to be situated in a sufficient elevation enabling a two-phase natural circulation mode, with both a condensing phase of the steam extracted from the steam generator, and a gravity draining return for the condensates to the steam generator. Such power extraction can be used for a relatively long period of time depending on the pool size.*

The present research is based on the use of a portion of the energy stored in this boiling water volume as a hot source for a thermodynamic cycle via an immersed heat exchanger. The power generated by this cycle will be used as an autonomous supply for various critical components, in addition to existing systems. This technology used here which can convert electricity from low-grade heat is similar with existing technologies already used for the valorization of renewable (biomass, solar, geothermal) or industrial waste heat at low and medium temperature (<150°C) into electricity.

An efficient technology is the organic Rankine cycle (ORC), which has been used at laboratory and industrial scales for about several decades. However, two major issues hamper the use of ORC in the context of PWR: the nature of the hot source (water at 100°C) and the requirement for system reliability and robustness. Aside from these two challenges, there are the usual constraints associated with this type of cycle: maximizing energy performance, using an environmentally friendly fluid, and minimizing space requirements.

An experimental test bench with a boiling water pool and an ORC with immersed evaporator was built to address this problem. The design of the immersed evaporator is explained, as well as the correlations used. The system reliability is then studied through the investigation of off-nominal situations (degraded heat transfer at ORC evaporator, “high” temperature of ORC condenser) for a first approach of reliability assessment. This study gives first elements for the demonstration of the adaptability of a partial admission axial micro-turbine to the variation of cold source temperature and to the entry of two-phase fluid in Novec649TM. All the experimental results will be used to validate the theoretical model of the ORC (condenser - evaporator - turbine) in order to design the ORC at scale 1.

I. Introduction

Nuclear power generates about 10% of global electricity, with approximately 450 nuclear power plants (NPP) [1], [2]. Three major nuclear accidents have occurred in recent decades: Three Mile Island (1979), Chernobyl (1986), and Fukushima Daiichi (2011) [3]–[5]. New generation NPPs (generation III and more) incorporate the state of the art of these accidents to improve safety systems.

Indeed, two major documents for advanced NPPs : the Advanced Light Water Reactor (LWR) Utility Requirements Document (URD) and the European Utility Requirements for LWR Nuclear Power Plants (EUR), provide requirement for safety design [6]–[8].

During the March 2011 Fukushima Daiichi NPP accident, two major issues caused the degradation of the usual safety systems: loss of off-site power due to the earthquake and loss of on-site power source due to the

tsunami [9]. These non-operational conditions result in a long period of loss of offsite power inducing a global loss of heat sink event, which causes core damage. As a result, a safety enhancement axe, focusing on passive safety systems for new-generation NPPs has been developed. Those systems can operated during station blackouts (SBO).

The strength of passive systems, such as passive residual heat removal system (PRHRS) relies on the absence on rotating machinery (such as pump or diesel): only natural forces, such as natural convection are used to transfers the core residual heat to the cold source (water or air). The use of passive system simplify plant systems and operation and maintenance [10].

Some new generation NPPs already include PRHRS [11]. This PRHRS can be connect directly to the primary loop as on the AP1000 [12] or the CAP140 [13]. Indeed, a PRHR transfers the residual heat from the core to the in-containment refuelling water storage tank (IRWST) through a heat exchanger (HX). To ensure natural convection, the IRWST is located above the reactor. Another existing solution is to connect the PRHRS through the secondary loop in order to cool the steam generator (SG) which removes the decay heat from the primary loop, as existing on the HPR1000 [14] or the CPR1000 [15]. This system is named secondary side passive residual heat removal system (SSPRHRS). Because the SSPRHRS is connected to the secondary side, the PRHR HX acts as a safety condenser (SACO).

However, due to water evaporation, the cooling time for a PRHR is determined by the total tank volume. The longer the cooling time, the larger the tank. For example, for the HPR1000, the total volume of the tank is supposed to be 2300 m³ to remove the residual heat over a 72-hour period [16].

These large volumes of water at sufficient heights can cause civil engineering issues as well as safety concerns. As a result, while passive cooling systems are effective and dependable, they should not be the only focus. Thus, another safety concern raised by various safety authorities is the installation of an emergency power supply in addition to the existing power supplies [17]. Then, one concept is to use the water tank as a hot source for a thermodynamic cycle such as a Stirling engine or an Organic Rankine Cycle (ORC). The electricity generated by the cycle will provide electricity for its own use (compressor) as well as a production surplus [18], [19]. The Fig. 2 illustrates the coupling of a PRHRS and an ORC.

ORC is a thermal-driven power cycle that generates electricity by using a heat source and a low-boiling-point

fluid as the working fluid [20], [21]. ORC has been identified as one of the best thermal engines for producing electricity with a low heat source (150 °C) [22]. The majority of the heat sources used are geothermal, with approximately 3 GW of cumulative installed capacity in 2020, with power output ranging from a few kW to several dozen MW [23].

Thus, despite the fact that ORC are a well-established system, their use in nuclear safety necessitates a focus on their reliability. Indeed, the ORC must be capable of producing electricity on any situation (extreme climatic conditions, aging of components etc.) continuously. To accomplish this, the article focuses on the design of an ORC, with an immersed evaporator on a boiling water tank.

II. Experimental bench design

The experimental test bench is composed of two main parts:

- The ORC composed of an immersed evaporator.
- The boiling water tank, which is supposed to replace the SACO pool, composed of heating rods, which are supposed to replace the operation of the passive SACO.

A picture of the coupling between the ORC and the boiling water tank is shown in Fig. 1. The test bench purpose is to act as a small-scale demonstrator and to enable scale transposition through the results obtained.



Fig. 1. ORC and boiling water tank

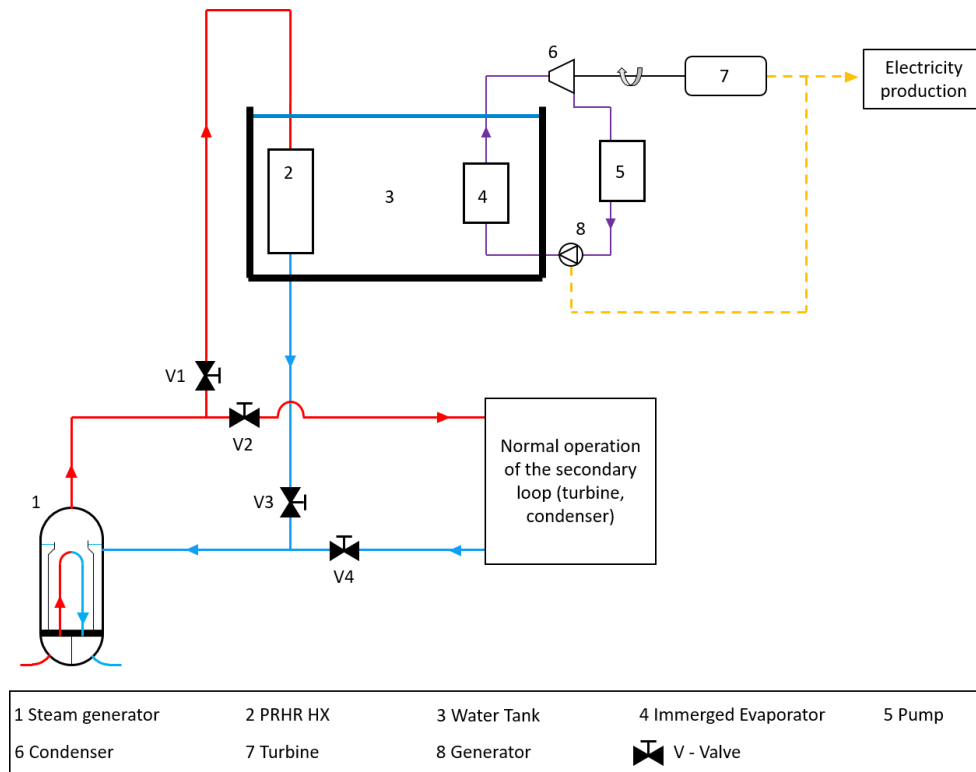


Fig. 2. PRHRS and ORC coupling - simplified diagram

The working fluid at the volumetric pump inlet is liquid. The working fluid is pumped to a high pressure level by the volumetric pump. The fluid is then heated in an immersed evaporator by the boiling water in the water tank. This vapor, at high temperature and pressure, is then expanded in a partial admission axial micro-turbine with a maximum power of about 1 kW. This expansion generates mechanical power, which is converted to electricity by a generator. Before returning to the pump, the low-pressure vapor is cooled by a plate condenser, which uses an active external water circuit as a cold source. A T-s diagram of the cycle is presented in Fig. 3.

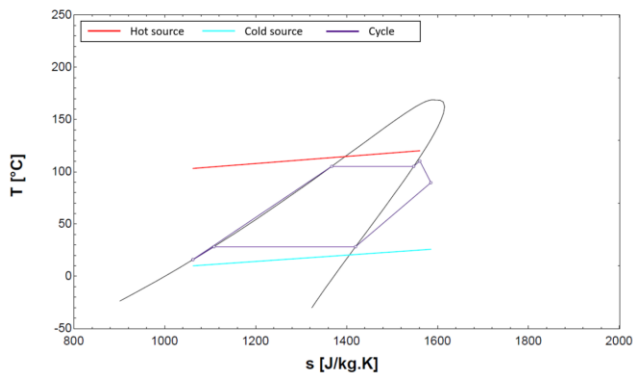


Fig. 3. T-s diagram of an ORC (Novvec649™)

The system lubrication is provided by the working fluid itself. An external circuit designed specifically for the generator keeps it cool. A small centrifugal pump is placed just before the volumetric pump to slightly increase the pressure and avoid cavitation. A tank, located between the condenser and the centrifugal pump, ensures a sufficient net positive suction head (NPSH) at the centrifugal pump inlet. An additional system comprised of a heat exchanger and a bypass system allows for the investigation of a wide range of cold source temperatures. The use of a pump in combination with a needle valve allows for the investigation of a wide range of mass flow rates and pressures.

The boiling water tank has a capacity of 1.5 m³. It includes ten 20 kW heating rods. Every heating rod has a heat flux density of 10.1 W/cm², which is roughly the same order of size as a SACO [24]. The power in the pool varies between 0 kW and 100 kW (five heating rods maximum). The maximum power ratio between heating rods and immersed exchanger is approximately five.

Temperature sensor rods are used to measure the temperature gradient in the tank. The positioning of the rods in the water tank are describe in Fig. 4. A level sensor system linked to an automatic valve controls the amount of water in the tank.

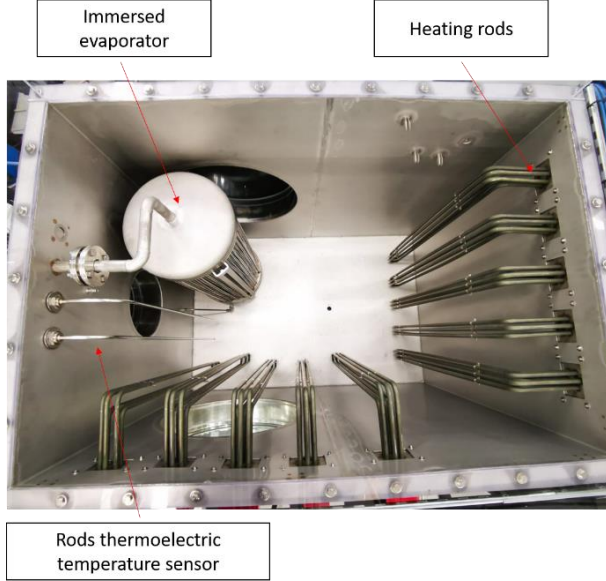


Fig. 4. Boiling water tank

III. Working fluid

The working fluid use in this work is the Novec649TM. This fluid is neither toxic nor flammable [25]. Furthermore, Novec649TM is exempt from the Kyoto and Paris agreements on refrigerant working fluids due to its environmental characteristics (ozone depletion potential (ODP) = 0 and global warming potential (GWP) = 1) (Table 1) [26], [27]. Moreover, Novec649TM is a dry fluid ($\partial T/\partial s > 0$) which avoid any risk of erosion on the turbine.

The thermodynamic properties of the Novec649TM, come from EES (engineering equation solver) software [28].

Table 1. Novec649TM properties

Properties	Novec649 TM
Fluid type	Dry
Fluid class	Fluoroketone
Formula	CF ₃ CF ₂ C(O)CF(CF ₃) ₂
Critical temperature (°C)	169
Critical pressure (bar)	18.7
Normal glide	0
ODP	0
GWP	1
Flammability	No
Toxicity	Null

IV. Evaporator design

The ORC immersed evaporator was designed to achieve two major goals: for the device to act as a small-scale demonstrator, and to validate experimentally inside and outside heat transfer coefficients. The validation of these models will enable a scale transposition via the conservation of some dimensionless numbers (Re; Ra).

The size of the experimental immersed evaporator is summarized in the Table 2.

Specification	Unit	Data
Length in height	[mm]	800
Distance between heat transfer tube	[mm]	18
Outside tube diameter	[mm]	3.17
Tube thickness	[mm]	0.89
Number of tubes	[-]	551
Total exchanger diameter	[mm]	406.4

Table 2 : Comparison of the parameters between scale 1 and experimental model.

In order to design the evaporator, a variety of correlations has been used, to characterize the exchanges inside and outside the tubes.

a. Natural convection

The Grashof number characterizes fluid movement in natural convection. In the case of constant heat flux, we can assume that the Grashof number is:

$$Gr^* = \rho^2 g \beta q \frac{d^4}{\lambda \mu^2} \quad (1)$$

The Rayleigh number is obtained by multiplying the Grashof number by the Prandtl number. This number describes natural convection. Natural convection experiments show that if the slenderness criterion is satisfied, the Rayleigh number must account for the effects of tube surfaces, i.e. the length and diameter of the tube [29]–[31]. It is transformed into:

$$Ra^* = Gr^* Pr \frac{D}{L} \quad (2)$$

Xu et al. (2021) [30], study the natural convection of a heat exchanger immersed into a pool acting as a hot source: 70 and 88 °C. They conclude that, in this situation, the best natural convection Nusselt correlation is given by Yang [32]:

$$Nu_{water} = 0.59 Ra^{*\frac{1}{3}} + 0.52 \quad (3)$$

This correlation is appropriate for turbulent Ra^* : between $0.0001 < Ra^* < 1.05 \cdot 10^6$.

Then, the external convection coefficient is calculated using:

$$\alpha_{water} = Nu_{water} * \frac{\lambda}{D} \quad (4)$$

The natural convection heat transfer between the wall and the water can thus be plotted as a function of Rayleigh (Fig. 5).

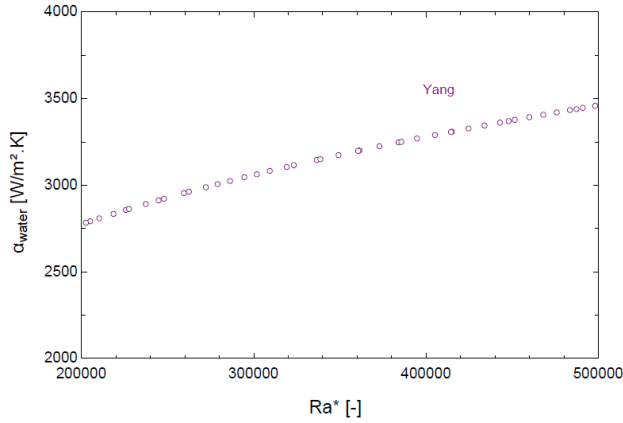


Fig. 5. α_{water} based on the Rayleigh

b. Forced convection

The following correlations were used inside the tubes in single phase:

During the preheating stage and for $Re < 2300$:

$$Nu = 4.36 \quad (5)$$

The correlation of Shah (1982) is then used during the evaporation phase [33]. This correlation is based on an enhancement factor. The correlation of Dittus and Boelter (1930) is first used to calculate the liquid heat transfer coefficient [34]. Then, the enhancement factor is defined as a function of the boiling number (Bo), the Froude number (Fr) and the convection number (Co).

$$\Psi = \frac{\alpha_{tf}}{\alpha_l} = f(Co; B; Fr) \quad (6)$$

This correlation estimates the two-phase heat transfer coefficient with an approximate value of 500 W/m².K. Thus two-phase heat transfer coefficients obtained in Novec649TM are of the same order of magnitude as those obtained for equivalent Reynolds numbers in the literature [35].

V. Turbine behaviour reliability

Because the ORC is designed to operate in an emergency situation, the reliability of its turbine is an important consideration in its design. To test this reliability, two situations have been tested.

First, consider the turbine behaviour as the temperature of the cold source rises. To accomplish this, the temperature of the cold source was experimentally varied between 13 and 35 °C to replicate the possible temperature variation of a water tank.

Then, the turbine acceptability to the presence of two-phase flow at the turbine inlet has been tested. The methodology was to increase the working fluid mass flow

rate until the evaporator could no longer evaporate the entire working fluid, forcing the entry of two-phase fluid into the turbine. The vapour quality of the working fluid has been reduced to 0.65 using this method. These experiments were carried out on an ORC, with a partial admission micro axial turbine, that was annexed to the one described in this article (Fig. 6). The fluid used is still Novec649TM.

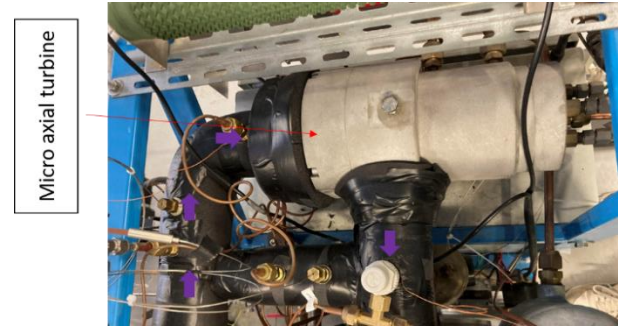


Fig. 6. Micro axial turbine of the experimental ORC

In nominal operation, the ORC can produce a power of about 450 W for an electrical efficiency of the turbine of about 27%. The nominal working point is presented on Table 3.

Parameters	Data	
Fluid	Novec649 TM	[-]
Mass flow rate	273.6	[kg.h ⁻¹]
Inlet temperature	108.2	[°C]
Inlet pressure	5.30	[bar]
Outlet pressure	0.44	[bar]
Rotation speed	9750	[RPM]

Table 3 : Design point

a. Cold source variation

As shown Fig. 7 as the temperature of the cold source decreases, so does the efficiency of the turbo generator. In fact, when the condensation pressure rises, the temperature of the cold source also rises. As a result, as the cold source temperature increase, the pressure ratio (eq (7)) decreases. This decrease of the pressure ratio reduces the electrical power produced by the turbo generator, and thus the efficiency of the turbo generator.

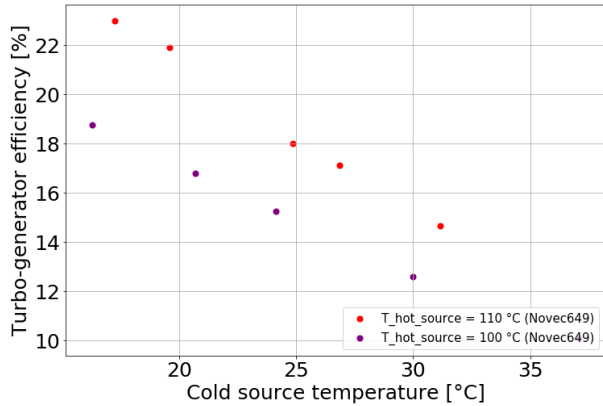


Fig. 7. Turbo-generator efficiency based on the cold source temperature

This effect of the cold source variation on the electrical output of the turbo-generator necessitates consideration of this variation during the design of the ORC at scale 1. Indeed, it is critical to ensure that the ORC can generate the required electrical power regardless of the temperature of the cold source. This requirement for consistency in production may result in a significant increase in the size of ORC organs.

b. Degraded heat transfer at ORC evaporator

The nominal point mass flow rate in Table 3 corresponds to the maximum power point in Fig. 8. After this point, the evaporator is unable to evaporate the entire working fluid, and the working fluid enters the turbine in two phases. The higher the mass flow rate, the lower the vapour quality. The power produced is 420 W for a vapour quality at the turbine inlet of 0.65, while the maximum power produced by the turbo-generator is 450 W, representing a 6.4% decrease. It is thus interesting to note that, even in the two-phase state, the turbo-generator continues to produce electrical power, with a slight decrease in comparison to the power produced in single phase.

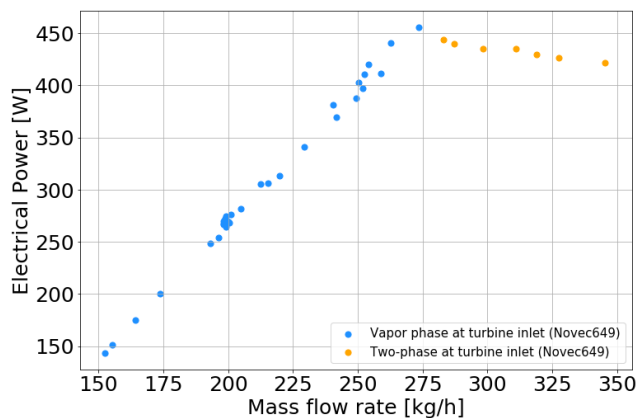


Fig. 8. Electrical power based on the ORC mass flow rate (single phase and two phase).

In Fig. 9, we can see that for single-phase test, the electrical efficiency of the turbo-generator increases as the power produced increases. We can also see that the single-phase efficiency is higher than the two-phase efficiency for any power. When, at the turbine inlet, the working fluid transitions from single-phase to two-phase, the turbo-generator efficiency decreases depending on the vapour quality. Reducing vapour quality from 1 to 0.65 results in a four-point decrease in turbo-generator efficiency. As a result, even if the turbo-generator continues to generate power with a two-phase fluid flow, the efficiency of the turbo-generator in two phases will always be lower than the efficiency of the single-phase turbo-generator.

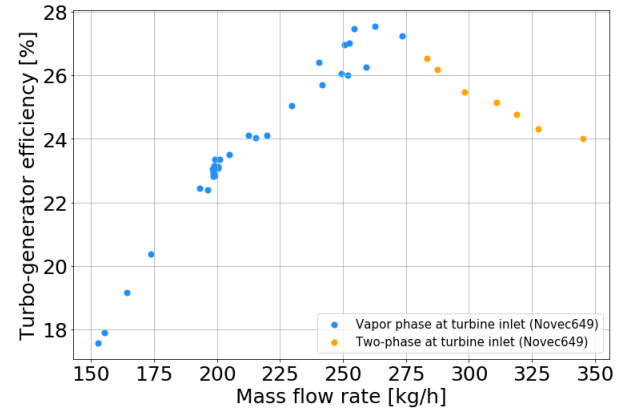


Fig. 9. Turbo-generator efficiency based on of the mass flow rate

In general, these results show that the ORC has a high degree of adaptability to a two-phase fluid condition at the turbine inlet. Although the electrical efficiency of the turbo-generator in two-phase is lower than in single-phase, the turbo-generator still produces significantly.

Thus, this turbine appears to be appropriate within the context of an experimental ORC representing as a small-scale demonstrator for nuclear safety. Indeed, despite being designed to operate in a single phase, this turbine accepts a degraded two-phase operation. This acceptability allows for the consideration of unexpected situations, such as the fouling of the immersed evaporator, which would result in a decrease in the evaporator thermal power.

c. Scaling

A correlation of the turbo-generator efficiency was created with the goal of changing the scale. The specific speed (N_s) and pressure ratio (π), two standard dimensionless turbomachinery parameters, are used to calculate this correlation (eq (7) and (8)). Using these two dimensionless parameters, it was possible to determine a correlation between the electrical efficiency of the turbo-generator for single-phase tests in Novtec649™.

The goal of this correlation is to account for both the turbine nominal and off-nominal situations such as the effect of cold source temperature or the entry of two-phase working fluid into the turbine.

$$\pi = \frac{P_{in,turb,total}}{P_{out,turb,static}} \quad (7)$$

$$N_s = N_{rota} \cdot \frac{\sqrt{Q_{out,1s}}}{\Delta h_{is}^{0.75}} \quad (8)$$

$$\eta_{turb} = a \cdot N_s + b \cdot N_s^2 + \frac{c}{\pi} + \frac{d}{\pi^2} + e \cdot (1 - x_{in,turb}) \quad (9)$$

This empirical correlation was set up with all the tests, with a range of validity of fluid vapour quality between 0.5 and 1 within a range of three points of efficiency.

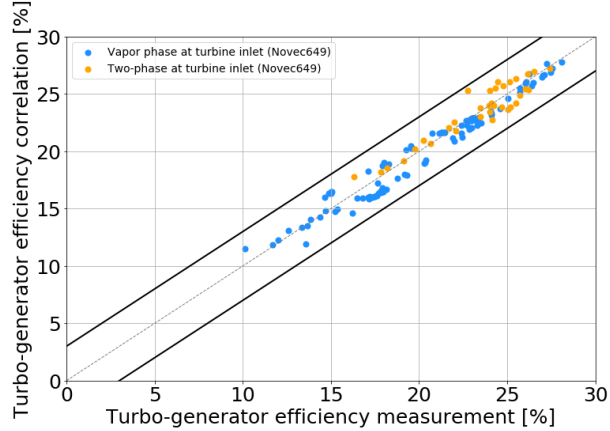


Fig. 10. Turbo-generator efficiency correlation based on turbo-generator efficiency measurement (single and two phase).

A more detailed study of this turbine in a multi-fluidic aspect is available [36].

VI. CONCLUSIONS

The goal of the ORC is to provide an independent source of electricity in the event of an unintentional SBO situation. This operating framework necessitates the design of a non-conventional ORC. Indeed, because it is immersed in a saturated water bath, its evaporator must operate via natural convection. Furthermore, these components must be able to work in non-nominal situations in order to demonstrate the system reliability.

A bibliographical study enabled the most appropriate correlations in natural convection according to a modified Rayleigh to be proposed, allowing the dimensioning of this immersed evaporator.

To address the issue of reliability, an ORC turbine, which is a critical component of its operation, was experimentally studied. This study provides first element to the demonstration of the adaptability of an axial micro-turbine with partial admission to the variation of the cold source and the entry of two-phase fluid into the stator. These experimental tests enabled the development of a correlation of the turbine operation in nominal and off-nominal situations.

The coupling with a boiling water tank and an ORC will then be subjected to experimental tests. These experimental tests will, first, be used as a small scale test rig to give elements for the demonstration of the functionality of the global system. In a second time, these experimental results will be used for the validation of the numerical models. These numerical models will allow the system to be scaled in order to design the ORC at scale 1.

ACKNOWLEDGMENTS

The authors would like to express their gratitude to the Atomic Energy and Alternative Energies Commission (CEA) and Electricité de France (EDF).

NOMENCLATURE

Symbols

d	tube diameter	[m]
g	acceleration of gravity	[m/s ²]
h	enthalpy	[J.kg ⁻¹]
L	tube length	[m]
N	rotation speed	[RPM]
P	pressure	[Pa]
q	heat flux	[W/m ²]
Q	volume flow	[m ³ /s]
x	vapour quality	[-]

Greek letters

α	heat transfer coefficient	[W/m ² .K]
β	coefficient of thermal expansion	[K ⁻¹]
Δ	difference	[-]
λ	thermal conductivity	[W/m.K]
μ	dynamic viscosity	[Pa.s]
π	pressure ratio	[-]
Ψ	enhancement ratio	[-]
ρ	density	[kg/m ³]

Dimensionless number

Bo	boiling number	[-]
Co	convective number	[-]
Fr	Froude number	[-]
Gr^*	Grashof number	[-]
Ns	specific speed	[-]
Nu	Nusselt number	[-]
Pr	Prandtl number	[-]
Ra^*	Rayleigh number	[-]
Re	Reynolds number	[-]

Subscripts

in	input
is	isentropic
l	liquid
out	output
rota	rotation
tf	two-phase
turb	turbine

Abbreviations

EES	engineering equation solver
-----	-----------------------------

EUR	European utility requirements
GWP	global warming potential
HX	heat exchanger
IRWST	in-containment refuelling water storage tank
LWR	light water reactor
NPSH	net positive suction head
NPP	nuclear power plants
ODP	ozone depletion potential
ORC	organic Rankine cycle
PRHRS	passive residual heat removal system
SACO	safety condenser
SBO	station blackouts
SG	steam generator
SSPRHRS	secondary side passive residual heat removal system
URD	utility requirements document

REFERENCES

- [1] ‘Nuclear Power Today | Nuclear Energy - World Nuclear Association’. <https://www.world-nuclear.org/information-library/current-and-future-generation/nuclear-power-in-the-world-today.aspx> (accessed Nov. 28, 2022).
- [2] ‘95/06080 Energy, electricity and nuclear power estimates for the period up to 2015’, *Fuel Energy Abstr.*, vol. 36, no. 6, p. 430, Nov. 1995, doi: 10.1016/0140-6701(95)95132-6.
- [3] G. R. Skillman and J. L. Rempe, ‘The Three Mile Island Unit 2 Accident’, in *Encyclopedia of Nuclear Energy*, E. Greenspan, Ed. Oxford: Elsevier, 2021, pp. 17–29. doi: 10.1016/B978-0-12-409548-9.12146-3.
- [4] A. R. Sich, ‘The Chernobyl Nuclear Power Plant Unit-4 Accident’, in *Encyclopedia of Nuclear Energy*, E. Greenspan, Ed. Oxford: Elsevier, 2021, pp. 30–52. doi: 10.1016/B978-0-12-819725-7.00080-5.
- [5] Internationale Atomenergie-Organisation, Ed., *The Fukushima Daiichi accident*. Vienna, Austria: International Atomic Energy Agency, 2015.
- [6] J. Xing, D. Song, and Y. Wu, ‘HPR1000: Advanced Pressurized Water Reactor with Active and Passive Safety’, *Engineering*, vol. 2, no. 1, pp. 79–87, Mar. 2016, doi: 10.1016/J.ENG.2016.01.017.
- [7] International Atomic Energy Agency, ‘International conference on fifty years of nuclear power - The next fifty years Book of extended synopses’, International Atomic Energy Agency (IAEA), 2004.
- [8] ‘Advanced Light Water Reactor Utility Requirements Document, Volume 1, Revision 2: ALWR Policy and Summary of Top-Tier Requirements’. <https://www.epri.com/research/products/TR-016780-V1R2> (accessed Nov. 30, 2022).
- [9] W. Luangdilok and P. Xu, ‘Chapter 5 - Nuclear plant severe accidents: challenges and prevention’, in *Advanced Security and Safeguarding in the Nuclear Power Industry*, V. Nian, Ed. Academic Press, 2020, pp. 99–134. doi: 10.1016/B978-0-12-818256-7.00005-2.
- [10] T. L. Schulz, ‘Westinghouse AP1000 advanced passive plant’, *Nucl. Eng. Des.*, vol. 236, no. 14, pp. 1547–1557, Aug. 2006, doi: 10.1016/j.nucengdes.2006.03.049.
- [11] J. Li *et al.*, ‘Experimental investigation on the heat removal capacity of secondary side passive residual heat removal system for an integrated reactor’, *Appl. Therm. Eng.*, vol. 204, p. 117973, Mar. 2022, doi: 10.1016/j.applthermaleng.2021.117973.
- [12] S. Estévez-Albuja, G. Jiménez, and C. Vázquez-Rodríguez, ‘AP1000 IRWST numerical analysis with GOTHIC’, *Nucl. Eng. Des.*, vol. 372, p. 110991, Feb. 2021, doi: 10.1016/j.nucengdes.2020.110991.
- [13] Y. Q. Li *et al.*, ‘Analyses of ACME integral test results on CAP1400 small-break loss-of-coolant-accident transient’, *Prog. Nucl. Energy*, vol. 88, pp. 375–397, Apr. 2016, doi: 10.1016/j.pnucene.2016.01.012.
- [14] D. C. Sun, Y. Li, Z. Xi, Y. F. Zan, P. Z. Li, and W. B. Zhuo, ‘Experimental evaluation of safety performance of emergency passive residual heat removal system in HPR1000’, *Nucl. Eng. Des.*, vol. 318, pp. 54–60, Jul. 2017, doi: 10.1016/j.nucengdes.2017.04.003.
- [15] M. Wang, H. Zhao, Y. Zhang, G. Su, W. Tian, and S. Qiu, ‘Research on the designed emergency passive residual heat removal system during the station blackout scenario for CPR1000’, *Ann. Nucl. Energy*, vol. 45, pp. 86–93, Jul. 2012, doi: 10.1016/j.anucene.2012.03.004.
- [16] D. C. Sun, Y. Li, Z. Xi, Y. F. Zan, P. Z. Li, and W. B. Zhuo, ‘Experimental evaluation of safety performance of emergency passive residual heat removal system in HPR1000’, *Nucl. Eng. Des.*, vol. 318, pp. 54–60, Jul. 2017, doi: 10.1016/j.nucengdes.2017.04.003.
- [17] *Éléments de sûreté nucléaire - Les réacteurs de recherche*. EDP Sciences, 2019. doi: 10.1051/978-2-7598-2301-7.
- [18] K. P. Singh, H. Sound, I. Rampall, C. Hill, and J. Rajkumar, ‘(54) Autonomous self-powered system for removing thermal energy from pools of liquid heated by radioactive materials, and method of the same’, p. 14.
- [19] E. Tatli, J. G. Belechak, B. Lu, C. Stansbury, C. Guler, and M. J. Ostrosky, ‘(54) Power generation from decay heat for spent nuclear fuel pool cooling and monitoring’, p. 7.
- [20] M. Astolfi, ‘3 - Technical options for Organic Rankine Cycle systems’, in *Organic Rankine Cycle (ORC) Power Systems*, E. Macchi and M. Astolfi, Eds. Woodhead Publishing, 2017, pp. 67–89. doi: 10.1016/B978-0-08-100510-1.00003-X.

- [21] J. B. Obi, 'State of Art on ORC Applications for Waste Heat Recovery and Micro-cogeneration for Installations up to 100kWe', *Energy Procedia*, vol. 82, pp. 994–1001, Dec. 2015, doi: 10.1016/j.egypro.2015.11.857.
- [22] N. Tauveron, S. Colasson, and J.-A. Gruss, 'Available systems for the conversion of waste heat to electricity', presented at the ASME International Mechanical Engineering Congress and Exposition, Proceedings (IMECE), 2014, vol. 6A. doi: 10.1115/IMECE2014-37984.
- [23] C. Wieland, F. Dawo, C. Schiffechner, and M. Astolfi, 'Market report on organic rankine cycle power systems: recent developments and outlook', p. 10, 2021.
- [24] B.-U. Bae, B.-J. Yun, S. Kim, and K. H. Kang, 'Design of condensation heat exchanger for the PAFS (Passive Auxiliary Feedwater System) of APR+ (Advanced Power Reactor Plus)', *Ann. Nucl. Energy*, vol. 46, pp. 134–143, Aug. 2012, doi: 10.1016/j.anucene.2012.03.029.
- [25] '3m-novec-engineered-fluid-649.pdf'. Accessed: Jan. 07, 2022. [Online]. Available: <https://multimedia.3m.com/mws/media/569865O/3m-novec-engineered-fluid-649.pdf>
- [26] *Proposal for a Regulation of the european parliament and of the council on fluorinated greenhouse gases*. 2012. Accessed: May 30, 2022. [Online]. Available: <https://eur-lex.europa.eu/legal-content/EN/ALL/?uri=celex%3A52012PC0643>
- [27] 'United Nations Climate Change, Kyoto Protocol Reference Manual on Accounting of Emissions and Assigned Amounts, 2008'. Accessed: Jan. 06, 2022. [Online]. Available: https://unfccc.int/resource/docs/publications/08_unfccc_kp_ref_manual.pdf
- [28] 'EES: Engineering Equation Solver | F-Chart Software : Engineering Software'. <https://fchartsoftware.com/ees/> (accessed Jul. 12, 2021).
- [29] C. O. Popiel and J. Wojtkowiak, 'Experiments on free convective heat transfer from side walls of a vertical square cylinder in air', *Exp. Therm. Fluid Sci.*, vol. 29, no. 1, pp. 1–8, Dec. 2004, doi: 10.1016/j.expthermflusci.2003.01.002.
- [30] J. Xu, X. Xie, M. Ding, C. Yan, and G. Fan, 'A one-dimensional code of double-coupled passive residual heat removal system for the swimming pool-type low-temperature heating reactor', *Nucl. Eng. Des.*, vol. 374, p. 111070, Apr. 2021, doi: 10.1016/j.nucengdes.2021.111070.
- [31] D. Lu, Y. Zhang, X. Fu, Z. Wang, Q. Cao, and Y. Yang, 'Experimental investigation on natural convection heat transfer characteristics of C-shape heating rods bundle used in PRHR HX', *Ann. Nucl. Energy*, vol. 98, pp. 226–238, Dec. 2016, doi: 10.1016/j.anucene.2016.08.009.
- [32] 'Yang, S. (1980). Free convections of heat outside slender vertical cylinders and inside vertical tubes. *Journal of Xi 'an Jiaotong University*, 14(3), 115-131.'
- [33] M. M. Shah, 'Chart correlation for saturated boiling heat transfer: Equations and further study', *ASHRAE Trans.*, pp. 185–195, 1982.
- [34] F. W. Dittus and L. M. K. Boelter, 'Heat transfer in automobile radiators of the tubular type', *Int. Commun. Heat Mass Transf.*, vol. 12, no. 1, pp. 3–22, Jan. 1985, doi: 10.1016/0735-1933(85)90003-X.
- [35] Q. Blondel, N. Tauveron, G. Lhermet, and N. Caney, 'Zeotropic mixtures study in plate heat exchangers and ORC systems', *Appl. Therm. Eng.*, vol. 219, p. 119418, Jan. 2023, doi: 10.1016/j.applthermaleng.2022.119418.
- [36] G. Lhermet, N. Tauveron, N. Caney, Q. Blondel, and F. Morin, 'A Recent Advance on Partial Evaporating Organic Rankine Cycle: Experimental Results on an Axial Turbine', *Energies*, vol. 15, no. 20, Art. no. 20, Jan. 2022, doi: 10.3390/en15207559.